

Supporting Information

Modulating Electrochemical Interfaces in CoFe@N-doped Carbon/Reduced Graphene Sheets for Enhanced Oxygen Evolution Reaction

Fanhao Kong[#], Kunfeng Chen[#], Shuyan Song^{*} and Dongfeng Xue^{*}

State Key Laboratory of Rare Earth Resource Utilization, Changchun Institute of Applied Chemistry, Chinese Academy of Sciences, Changchun 130022, China

[#]Authors with same contribution.

^{*}Corresponding author. E-mail: songsy@ciac.ac.cn, dongfeng@ciac.ac.cn

Experimental

Materials: All chemicals used were of analytical grade and used directly without further treatment. Potassium hydroxide (KOH, 85%) was purchased from Beijing Chemical Works, Potassium hexacyanoferrate ($K_4[Fe(CN)_6]$, 99.5%) and Cobaltous chloride hexahydrate ($CoCl_2 \cdot 6H_2O$, 98%) was from Xilong Chemicals Co. Ltd., Nafion solution (5%) from Alfa Aesar and Ruthenium (IV) oxide (RuO_2 , 99.9%) from Aladdin Industrial Corporation.

Synthesis of GO solutions: GO solutions (5 mg mL^{-1}) were synthesized according to our previous work.

Synthesis of $Co_2[Fe(CN)_6]/GO$ and $Co_2[Fe(CN)_6]$: In a typical synthesis of $Co_2[Fe(CN)_6]/GO$, 25 mL of GO solutions were added into a beaker under magnetic stirring for 20 min at room temperature. Then, 10 mL of $K_4Fe(CN)_6 \cdot 3H_2O$ (0.05 M) aqueous solutions were put slowly into GO solutions at rate of one drop per second. After continuous magnetic stirring for 1 h, 10 mL of $CoCl_2 \cdot 6H_2O$ (0.10 M) aqueous solutions were added into above mixtures, followed by mixing for additional 1h to form the homogenous precursor suspensions. The homogenous precursor suspensions were aged for 10 h under ambient condition. 20 mL of as-obtained precursor suspensions were transferred into a suction flask with a diameter of 10 cm, followed by repeatedly washing with DI water and dried at $60 \text{ }^\circ\text{C}$ in an oven. This sample contained $Co_2[Fe(CN)_6]$ nanocomposites supported by GO sheets and is thus denoted as $Co_2[Fe(CN)_6]/GO$. The $Co_2[Fe(CN)_6]$ sample was synthesized as same as $Co_2[Fe(CN)_6]/GO$ instead of equal volume of DI water was added to reaction system

without the introduction of GO. The $\text{Co}_2[\text{Fe}(\text{CN})_6]$ free GO sample is denoted as $\text{Co}_2[\text{Fe}(\text{CN})_6]$.

Synthesis of CoFe@NC/rGO and CoFe@NC : Above obtained $\text{Co}_2[\text{Fe}(\text{CN})_6]/\text{GO}$ and $\text{Co}_2[\text{Fe}(\text{CN})_6]$ were annealed in muffle furnace at 800°C for 1 h under the protection of N_2 at a heating rate of 5°C min^{-1} . The obtained samples are denoted as CoFe@NC/rGO and CoFe@NC , respectively. In addition, the $\text{Co}_2[\text{Fe}(\text{CN})_6]/\text{GO}$ was also annealed at 600, 700, and 900°C for 1 h under the protection of N_2 at a heating rate of 5°Cmin^{-1} .

Characterization: X-ray diffraction (XRD) was conducted on a Bruker D8 Focus diffractometer with $\text{Cu K}\alpha$ radiation ($\lambda = 0.15418\text{nm}$). Microstructure observation was measured on a Hitachi S4800 scanning electron microscope (SEM) at an accelerating voltage of 10 kV and a FEI Tecnai F20 transmission electron microscope (TEM) at an accelerating voltage of 200 kV. Raman spectra were performed on a DXRxi micro Raman system with a 532nm laser excitation. Four points probe resistivity measurements were tested on the Keithley 2400 Source Meter. Thermogravimetric analysis (TGA) was measured on an ETZSCH STA 449F3 Jupiter from 25 to 1000°C at a ramp rate of 5°C min^{-1} under N_2 atmosphere. The BET surface area, pore volume, and pore diameter were carried out on an ASAP 2020 surface area and porosity analyzer under liquid nitrogen condition. The surface chemical composition and valence of sample was investigated by X-ray photoelectron spectroscopy (Thermo ESCALAB 250).

Measurements: All of the electrochemical measurements were carried out on a CHI660D potentiostat (CH Instruments, Shanghai) containing a three-electrode system using a graphite rod as counter electrode, a saturated calomel electrode (SCE) as reference electrode, and a catalyst modified glassy carbon electrode (GCE, $d = 3\text{ mm}$) as measuring electrode in 1 M KOH aqueous solution at room temperature. To prepare measuring electrode, 3.5 mg of catalyst was put into 490 μL of mixed solvent ($V_{\text{water}}:V_{\text{ethanol}} = 1 : 1$) with the addition of 10 μL of 5 wt% Nafion solution, followed by sonication for 1 h to form a homogeneous ink. Then, 8 μL of ink was dropped onto GCE and dried naturally. The OER performance of samples were estimated by linear scan voltammetry (LSV) plots range from 0 to 0.65 V with a scan rate of 2 mVs^{-1} . EIS were performed at 1.55 V vs RHE with frequency range from 0.01 Hz to 100 KHz. Long-term stability of catalysts was measured by chronoamperometry, while the potential cycling stability was performed by exerting continuous cyclic voltammograms with a scan rate 100 mVs^{-1} . All of the potentials were showed vs. the reversible hydrogen electrode (RHE). In 1 M KOH, $E_{\text{RHE}} = E_{\text{SCE}} + 0.241\text{ V} + 0.059 \times \text{pH}$. Electrochemical measurements in this work were conducted without iR-correction.

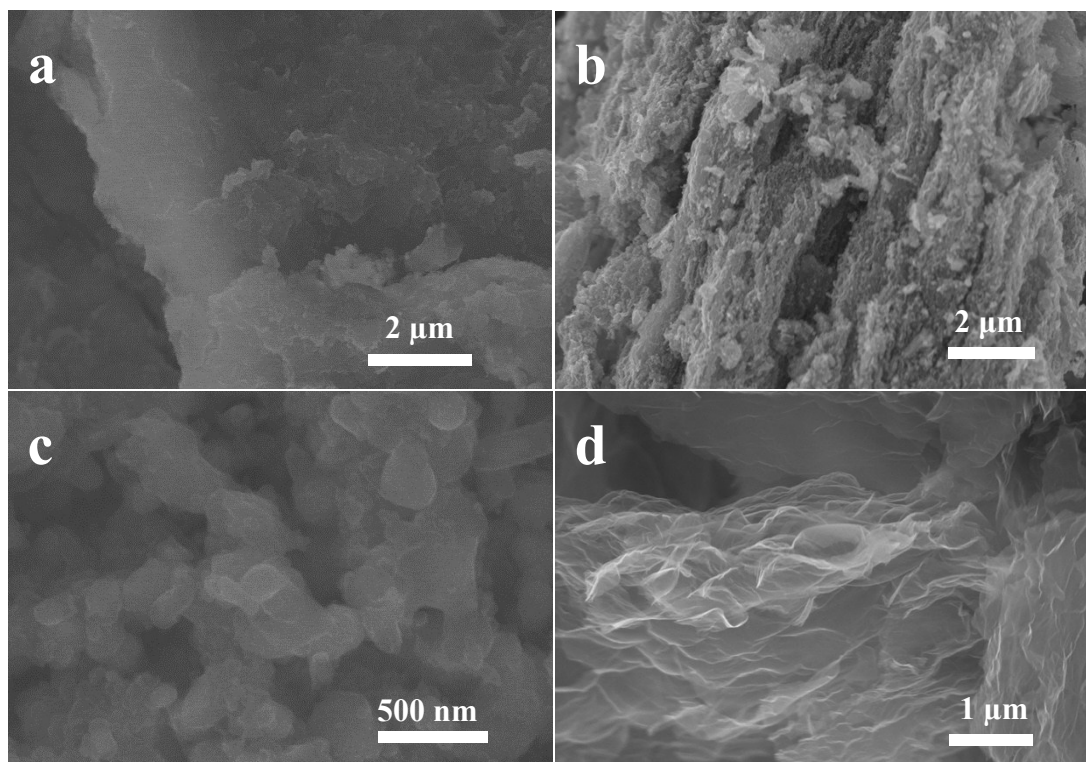


Figure S1. SEM images of the as-precursor $\text{Co}_2[\text{Fe}(\text{CN})_6]/\text{GO}$ (a), $\text{CoFe}@ \text{NC}/\text{rGO}$ (b), $\text{CoFe}@ \text{NC}$ (c), and rGO (d).

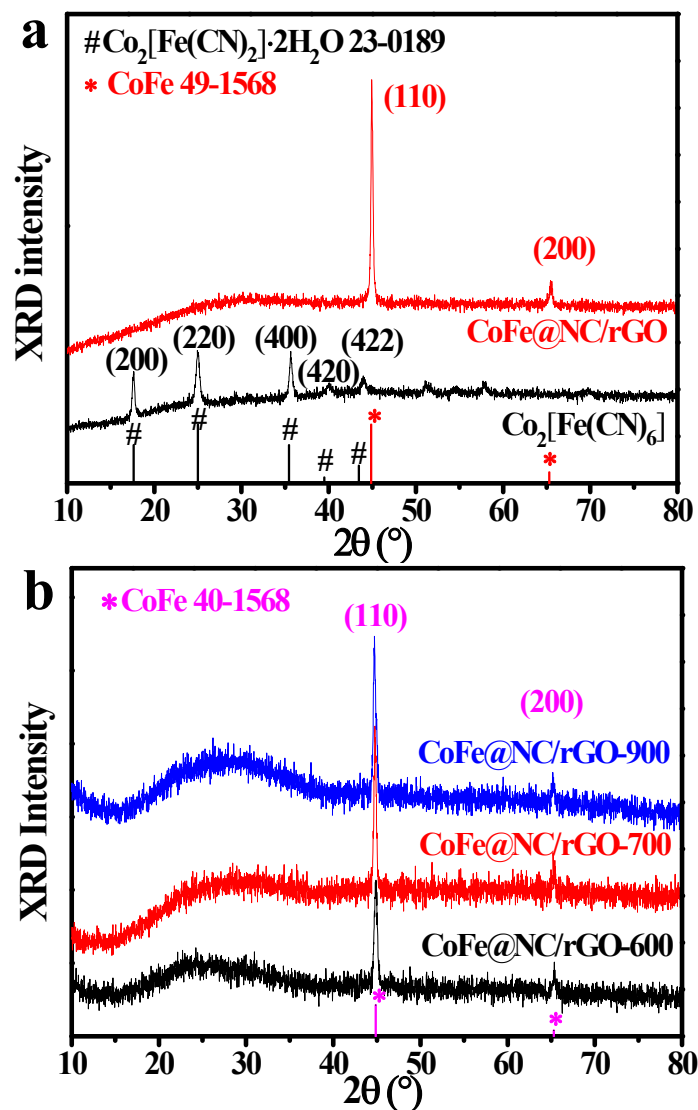


Figure S2. XRD patterns of (a) the CoFe@NC and Co₂[Fe(CN)₆]/GO, (b) various sandwich-like CoFe@NC/rGO obtained at different temperatures: 600, 700, and 900 °C.

Table S1. Comparison of OER performances with reported non-noble transition metal-based catalysts in basic electrolyte.

OER catalyst	Electrolyte	Overpotential (10 mAcm ⁻²)	Tafel slope (mVdec ⁻¹)	Reference
CoFe@NC/rGO	1 M KOH	278	52	This work
FeNi@NC/CNTs	1 M NaOH	280	70	1
NiFe@NC	1 M KOH	300	-	2
NiCo/PFC	0.1 M KOH	400	106	3
FeCoMo	1 M KOH	277	28	4
NiCo@NCNTs	0.1 M KOH	420	177	5
FeCoNi	1 M KOH	288	-	6
CCS Ni-Co NWs	1 M KOH	302	44	7
Ni ₂ Co ₁ @Ni ₂ Co ₁ O _x	1 M KOH	320	42	8
Ni-P	1 M KOH	300	64	9
FeNi LDH	1 M KOH	300	40	10
Ni ₃ C/C	1 M KOH	320	46	11
NiO/Ni	1 M KOH	345	53	12
Ni-Co mixed oxides	1 M KOH	380	50	13
UltrathinCo ₃ O ₄ /rGO	1 M KOH	290	68	14
CoNi(20:1)-P-NS	1 M KOH	280	45	15
Co ₃ O ₄ /rGO	1 M KOH	346	47	16
NiO/NiFe ₂ O ₄	1 M KOH	303	59	17

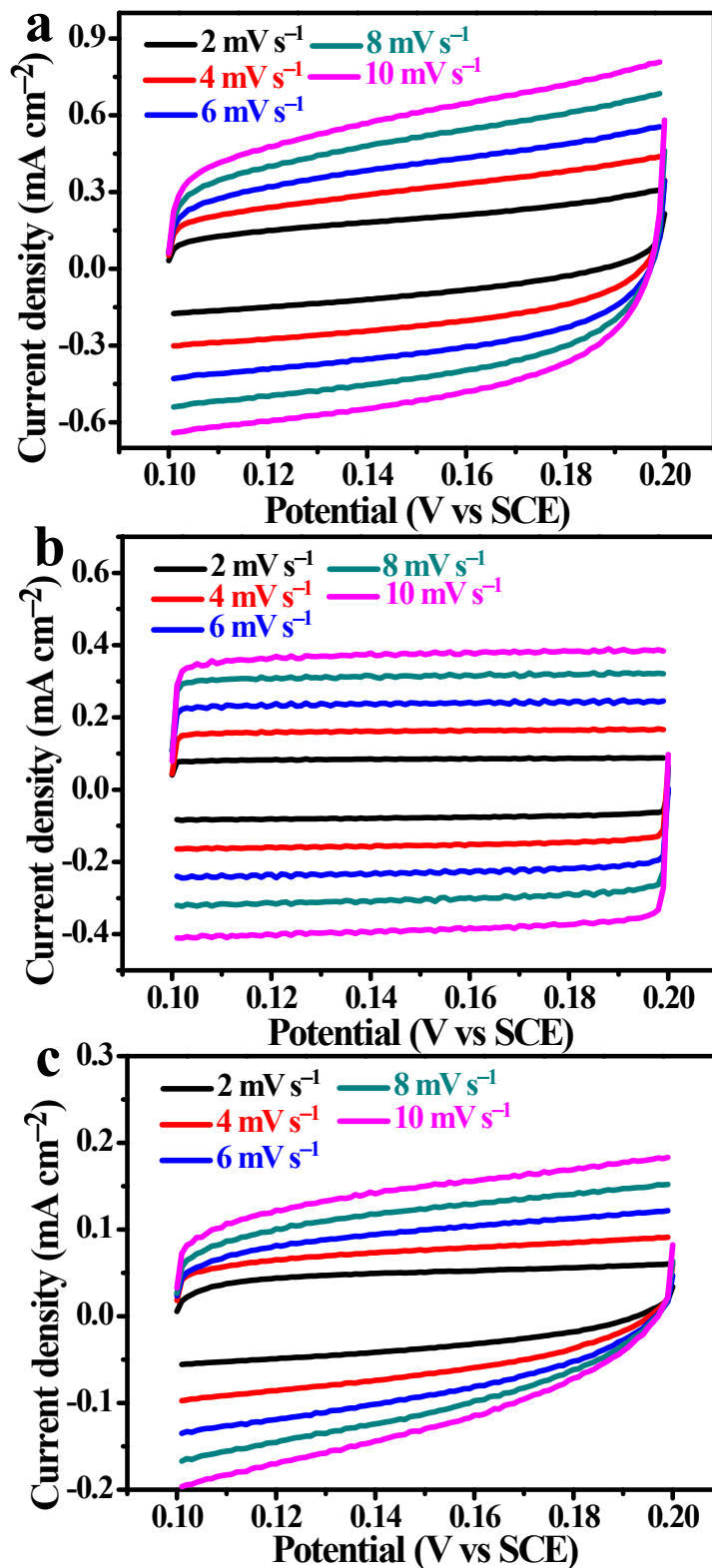


Figure S3. Cyclic voltammety curves for a) CoFe@NC/rGO, b) RuO₂, c) CoFe@NC modified-electrode from 2 mV s⁻¹ to 10 mV s⁻¹.

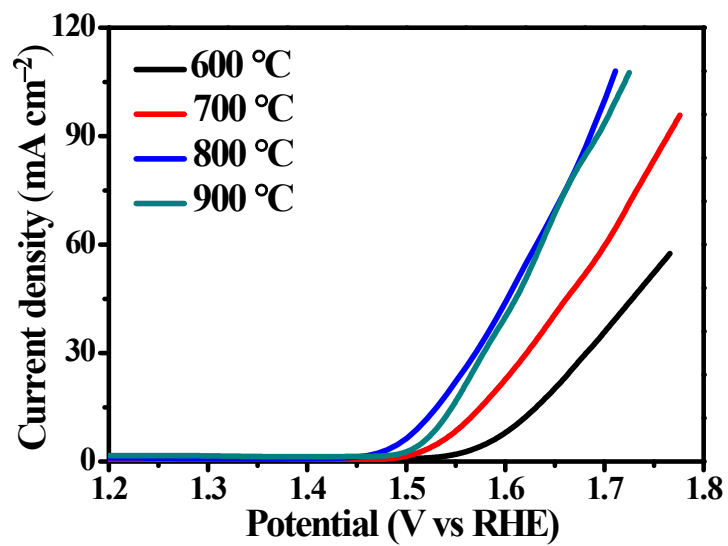


Figure S4. The OER polarization curves of sandwich-like CoFe@NC/rGO obtained at different annealing temperatures.

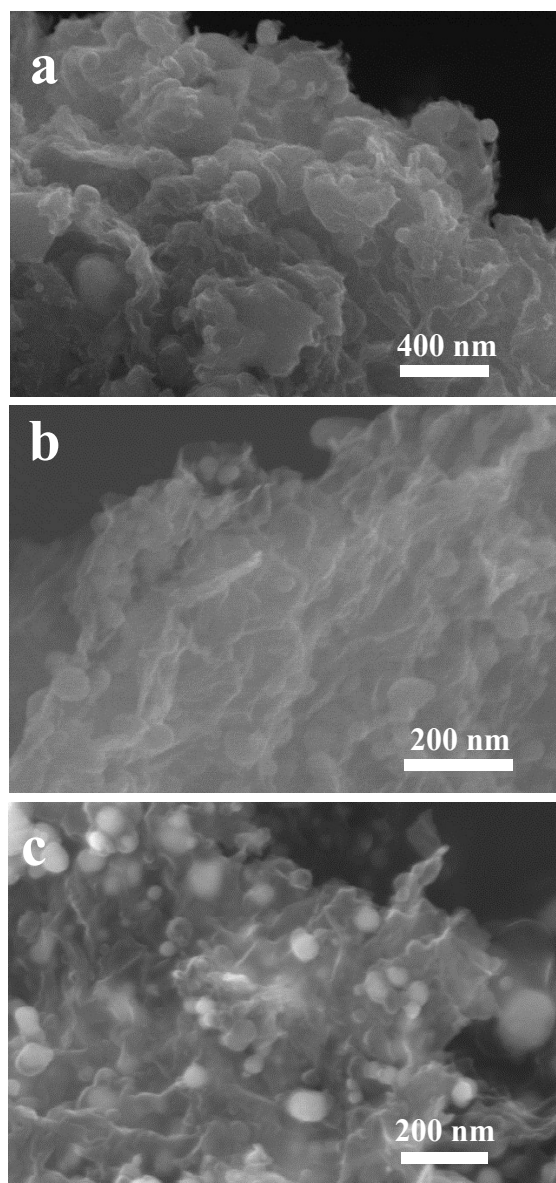


Figure S5. SEM images of sandwich-like (a) CoFe@NC/rGO-600, (b) CoFe@NC/rGO-700, and (c) CoFe@NC/rGO-900.

Table S2. Conductivity of four points probe resistivity measurements for sandwich-like CoFe@NC/rGO at different annealing temperatures.

Catalysts	600°C	700°C	800°C	900°C
Conductivity	6.43 S cm ⁻¹	16.60 S cm ⁻¹	76.10 S cm ⁻¹	92.85 S cm ⁻¹

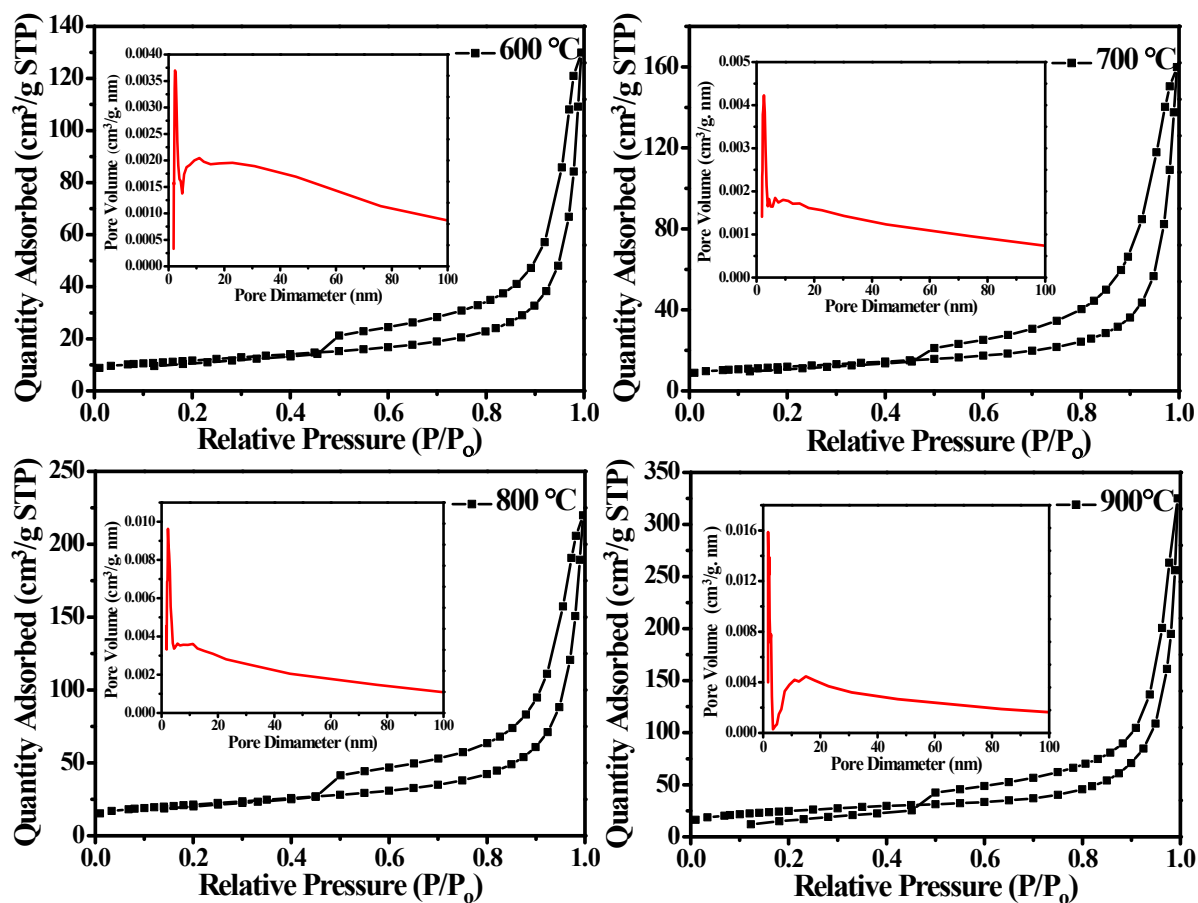


Figure S6. N₂ adsorption-desorption isotherm and the corresponding pore size distribution (the inset) of the sandwich-like CoFe@NC/rGO obtained at different annealing temperatures: 600, 700, 800, 900 °C.

Table S3. BET surface area and pore analysis of sandwich-like CoFe@NC/rGO at different annealing temperatures.

Catalysts	BET surface area/ $\text{m}^2 \text{g}^{-1}$	Total pore volume/ $\text{cm}^3 \text{g}^{-1}$	Pore diameter/ nm
600 °C	40.21	0.13	12.66
700 °C	39.15	0.10	10.57
800 °C	72.26	0.19	10.33
900 °C	84.56	0.25	11.80

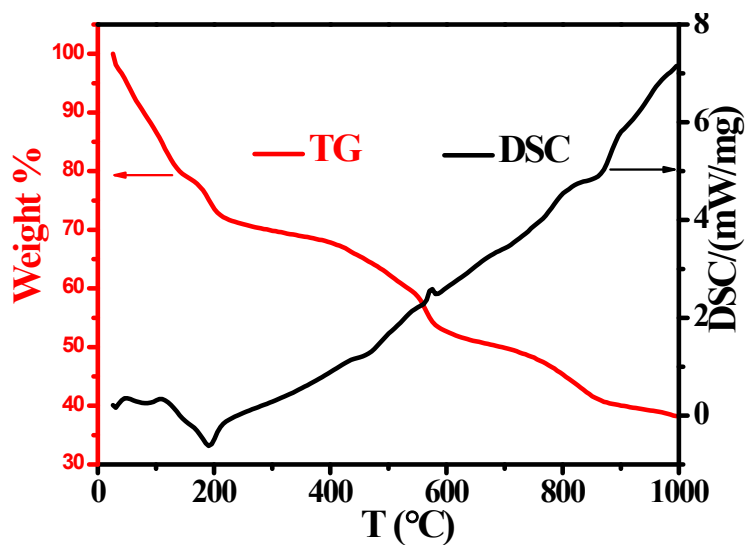


Figure S7. TGA (red) and its corresponding DSC (black) curves of $\text{Co}_2[\text{Fe}(\text{CN})_6]/\text{GO}$ under N_2 .

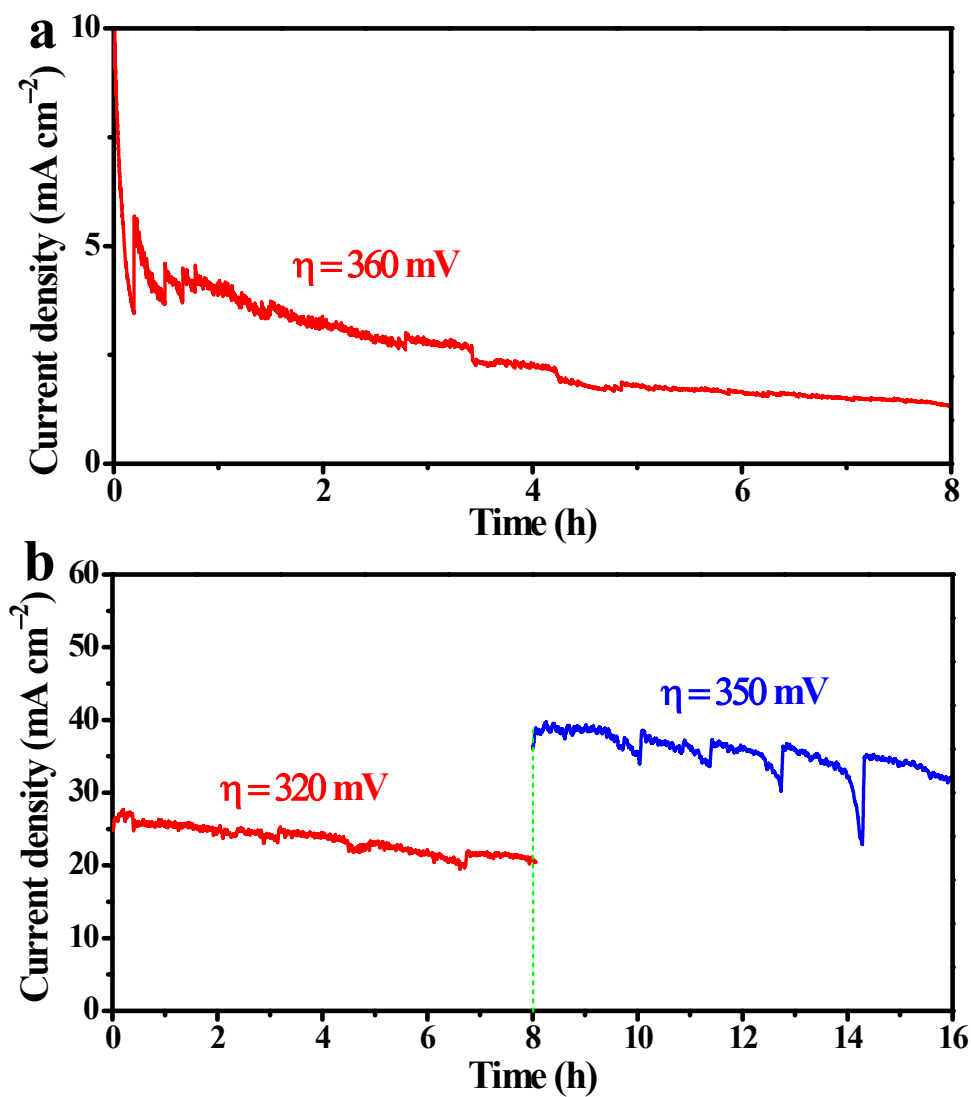


Figure S8. Long-term stability of (a) CoFe@NC at the overpotential of 360 mV, (b) sandwich-like CoFe@NC/rGO at the overpotentials of 320 mV and 350 mV.

References for support information

- 1 X. J. Cui, P. J. Ren, D. H. Deng, J. Deng, and X. H. Bao, *Energy Environ. Sci.*, 2016, 9, 123-129.
- 2 Z. P. Zhang, Y. S. Qin, M. L. Dou, J. Ji, F. Wang, *Nano Energy* 2016, 30, 426-433.

- 3 G. T. Fu, Y. F. Chen, Z. M. Cui, Y. T. Li, W. D. Zhou, S. Xin, Y. W. Tang, and J. B. Goodenough, *Nano Letters* 2016, 16, 6516-6522.
- 4 P. F. Liu, S. Yang, L. R. Zheng, B. Zhang, and H. G. Yang, *Chem. Sci.*, 2017, 8, 3484-3488.
- 5 J. Yu, Y. J. Zhong, W. Zhou, Z. P. Shao, *J. Power Sources* 2017, 338, 26-33.
- 6 Y. Yang, Z. Y. Lin, S. Q. Gao, J. W. Su, Z. Y. Lun, G. L. Xia, J. T. Chen, R. R. Zhang, and Q. W. Chen, *ACS Catal.* 2017, 7, 469-479.
- 7 S. H. Bae, J. E. Kim, H. Randriamahazaka, S. Y. Moon, J. Y. Park, H. -K. Oh, *Adv. Energy Mater.* 2017, 7, 1601492.
- 8 J. L. He, B. B. Hu, Y. Zhao, *Adv. Funct. Mater.* 2016, 26, 5998-6004.
- 9 X. -Y. Yu, Y. Feng, B. Y. Guan, X. W. (David) Lou, and U. Paik, *Energy Environ. Sci.* 2016, 9, 1246-1250.
- 10 F. Song, X. L. Hu, *Nat. Commun.* 2014, 5, 4477.
- 11 K. Xu, H. Ding, H. F. Lv, P. Z. Chen, X. L. Lu, H. Cheng, T. P. Zhou, S. Liu, X. J. Wu, C. Z. Wu, Y. Xie, *Adv. Mater.* 2016, 28, 3326-3332.
- 12 J. Y. Liang, Y. Z. Wang, C. C. Wang, and S. Y. Lu, *J. Mater. Chem. A*, 2016, 4, 9797-9806.
- 13 L. Han, X. Y. Yu, X. W. Lou, *Adv. Mater.* 2016, 28, 4601-4605.
- 14 Y. Y. Chen, J. Hu, H. L. Diao, W. J. Luo, and Y. F. Song, *Chem. Eur. J.* 2017, 23, 4010 -4016.
- 15 X. F. Xiao, C. T. He, S. L. Zhao, J. Li, W. S. Lin, Z. K. Yuan, Q. Zhang, S. Y. Wang, L. M. Dai, and D. S. Yu, *Energy Environ. Sci.*, 2017, 10, 893-899.
- 16 M. Leng, X. L. Huang, W. Xiao, J. Ding, B. H. Liu, Y. H. Du, J. M. Xue, *Nano Energy* 2017, 33, 445-452.
- 17 B. K. Kang, M. H. Woo, J. Lee, Y. H. Song, Z. L. Wang, Y. N. Guo, Y. Yamauchi, J. H. Kim, B. Lim, and D. H. Yoon, *J. Mater. Chem. A* 2017, 5, 4320-4324.